Effect of Clay Platelet Dispersion as Affected by the Manufacturing Techniques on Thermal and Mechanical Properties of PMMA-Clay Nanocomposites

A. K. Dhibar, S. Mallick, T. Rath, B. B. Khatua

Materials Science Centre, Indian Institute of Technology Kharagpur, Kharagpur 721302, India

Received 12 August 2008; accepted 13 March 2009
DOI 10.1002/app.30420
Published online 1 May 2009 in Wiley InterScience (www.interscience.wiley.com).

ABSTRACT: In this work, the properties of Poly(methyl methacrylate) (PMMA)-clay nanocomposites prepared by three different manufacturing techniques viz., solution mixing, melt mixing, and *in-situ* bulk polymerization in presence of clay were studied. Morphological analysis revealed that the extent of intercalation and dispersion of the nanoclay were relatively higher in the *in-situ* polymerized nanocomposites than those of solution and melt blended nanocomposites. Differential Scanning Calorimetric study indicated maximum increment in T_g of the PMMA in the *in-situ* polymerized PMMA-clay nanocomposites. Thermo gravimetric analysis showed improved thermal stability of PMMA in all the nanocomposites and the maximum improvement was for *in-situ* polymerized nanocomposites. The storage moduli of all the nanocomposites were higher than the pure PMMA. © 2009 Wiley Periodicals, Inc. J Appl Polym Sci 113: 3012–3018, 2009

Key words: polymer nanocomposites; intercalation; glass transition; storage modulus

INTRODUCTION

Polymer-clay nanocomposite has received considerable attention because of the potential of adding infinitesimally small clay platelets to dramatically raise mechanical, thermal and barrier properties without increasing the specific gravity or reducing the transparency of the base material.[1–7] The homogeneous dispersion of 3–5 wt % of nanoclay improves the mechanical and thermal properties of the polymer matrix to the same extent as with 30-50 wt % of micro-sized fillers.[8–11]

Poly(methyl methacrylate) (PMMA) has several desirable properties, including high strength, good weatherability, optical clarity, and excellent dimensional stability. PMMA-clay nanocomposite offers the potential for improved physical performance, increased heat resistance, and reduced gas permeability, without a sacrifice in optical clarity.[12–20] The literature contains several reports on the effect of the layered silicate on the properties of PMMA-clay nanocomposites, MMA polymerization behaviour rather than the effect of preparation method on the structure and properties of the final hybrid. Jiang et al.[12] studied the intercalation of high molecular weight PMMA into organic clay. Shen et al.[13] have reported increased thermal stability of melt-intercalated PMMA-clay nanocomposite compared with that of the neat PMMA, or of a physical mixture of PMMA and clay. Okamoto et al.[14] has reported improved storage modulus and glass transition temperature (T_g) of PMMA in *in-situ* intercalative free-radical polymerized PMMA-clay nanocomposite. Kim and Hwang[15] investigated the effect of pre-shearing on structure and properties of the *in-situ* polymerized PMMA-clay nanocomposites and reported an improved intercalation of the clay with pre-shearing time. Recently, Liqiang et al.[16] have studied the effect of modified clay on the morphology of *in-situ* polymerized PMMA-clay nanocomposites and reported increased modulus and tensile properties of the nanocomposite with the clay loading. Huang et al.[17] has synthesized intercalated PMMA-clay nanocomposite by suspension polymerization. Samal and Samal[18] have reported a significant improvement of thermal stability in emulsion polymerized PMMA-clay nanocomposite resulted from strong interactions between PMMA and dispersed clay layers. Natarajan et al.[19] have showed that the tensile modulus of melt-blended PMMA-clay nanocomposite increased linearly with the clay loading. Rajan et al.[20] have reported 30% increment of thermal stability of radical polymerized PMMA-clay nanocomposite followed by ultrasonic mixing compared to that of magnetic stirring. Yagci and coworkers[21] reported the extent of intercalation and thermal stability enhancement with clay loading in radical polymerized PMMA-clay nanocomposite using intercalated chain transfer agent.

Correspondence to: B. B. Khatua (khatuabb@matsc.iitkgp.ernet.in).

In summary, literature reports on preparation of PMMA-clay nanocomposite by various method and their characterizations. However, homogeneous dispersion of clay platelets in the PMMA matrix is still a major problem. In our present work, efforts have been put forward to prepare PMMA-clay nanocomposite by different manufacturing techniques, and to study the effect of clay platelets dispersion, as affected by preparation methods, on thermal and mechanical properties of PMMA-clay nanocomposite. Here, we focus on the details of our findings.

EXPERIMENTAL

Materials used

Methyl methacrylate (MMA) monomer used in this study was of synthesis grade and procured from Merck, Germany. Benzoyl peroxide (BP), chloroform and dichloromethane were supplied by Merck, Germany. The organoclay employed in this study was Cloisite 20A (Southern Clay Product). It is a montmorillonite modified with dimethyl dihydrogenated tallow ammonium to increase the domain (d) spacing of Na^+ montmorillonite. The cation exchange capacity (CEC) of Cloisite 20A is 95 mequiv/100 g. Hereafter, Cloisite 20A is referred to as the clay.

Preparation of PMMA-Clay nanocomposites

PMMA-Clay Nanocomposites were synthesized by three different manufacturing techniques followed by melt processing, as given below:

In-situ bulk polymerization followed by melt intercalation technique

A total of 130 ml MMA monomer was taken in a 500 ml separating funnel and NaOH solution was added into it. The mixture was shaken for 15 min and decants the purified MMA in a 250 ml beaker. This process was continued for 2-3 times. Finally, after washing with de-ionized water, the purified MMA was collected.

Purified MMA (100 ml) and clay (2 g) were taken in a 250 ml beaker. The mixture was allowed for ultrasonication at room temperature for 1 h to intercalate the monomer inside the clay platelets. A total of 100 mg benzoyl peroxide (BP) was added to the solution and stirred until dissolved. The reactor was kept in an oil bath and the temperature of the reactor was increased to 90°C. The reaction was carried out in nitrogen atmosphere for 40 min. The viscous PMMA solution was cooled at room temperature. The yield of the PMMA-clay nanocomposites was 66 g. Thus the effective clay loading in nanocomposites was calculated to be 3.03 wt %.

The PMMA-clay nanocomposite was then melt mixed in internal mixer at 220°C for 15 min at 60 rpm and compression molded at the same temperature under constant pressure. The PMMA was also synthesized by following the same bulk polymerization procedure with out adding any clay.

Solution blending followed by melt intercalation technique

A total of 50 g bulk polymerized PMMA was dissolved in 250 ml dichloromethane. A total of 1.5 g clay was added in to the solution and stirred for 30 min in a 500 ml beaker at room temperature. Finally, the solvent was allowed to evaporate. The resulting PMMA-clay nanocomposite was then melt mixed in internal mixer at 220°C for 15 min at 60 rpm and compression molded at the same temperature under constant pressure.

Direct melt processing technique

A total of 50 g bulk polymerized PMMA and 1.5 g clay were dry mixed. Then this PMMA-clay mixture was taken in internal mixer at 220°C. The mixing was carried out at 60 rpm for 15 min. The melt mixed PMMA-clay nanocomposite was cooled at room temperature and finally compression molded at the same temperature under constant pressure.

CHARACTERIZATION

Molecular weight determination by viscometric method

The viscosity average molecular weight of the neat PMMA and the PMMA in *in-situ* polymerized PMMA-clay nanocomposites were determined by viscometric method in chloroform, following the Mark-Houwink equation, as given below:

$$\eta = K M_v^a \quad (1)$$

Where η is the viscosity of the solution, $K = 0.34 \times 10^{-4}$ and $a = 0.83$ at 25°C for chloroform.

PMMA in the PMMA-clay nanocomposite was extracted by tetrahydrofuran (THF) using a Soxhlet extractor.

X-ray diffraction study

The d spacing of the layer structure of the clay itself as well as that in the composites was examined by using a wide-angle X-ray diffractometer (Rigaku XRD, Ultima-III, Japan) with nickel-filtered Cu Kα line ($\lambda = 0.154\ 04$ nm) operated at 40 kV $\times$ 100 mA and a scanning rate of 2 deg/min. The sample-to-detector distance was 400 mm.

TEM analysis

The extent of dispersion of the clay in the PMMA matrix was studied by transmission electron microscopy (TEM: CM 12, PHILIPS) operating at an accelerating voltage of 120 kV. Pure PMMA and PMMA-clay samples were ultra-microtomed at cryogenic condition with a thickness of ~50 nm. Since the clay has much higher electron density than neat polymers, it appeared dark in TEM images.

Thermo gravimetric analysis (TGA)

The thermal stability (onset degradation temperature and temperature corresponds to 50 wt % loss and maximum weight loss) of the neat PMMA and the composites was investigated with the help of thermo gravimetric analysis (TGA-209F, from NETZSCH). The sample was heated from room temperature to 600°C at a heating rate of 10°C/min under air atmosphere.

Differential scanning calorimetry (DSC)

The glass transition temperature (T_g) of the neat PMMA and the PMMA in the nanocomposites was determined with Differential Scanning Calorimetry (DSC-200 PC, NETZSCH). The second heating curves of the pure PMMA and PMMA-clay nanocomposites were taken for determination of T_g. The heating and cooling rate was 10°C/min.

Dynamic mechanical analyzer (DMA)

Dynamic modulus and glass transition temperature of the composites were measured in tension film mode at a constant vibration frequency of 1 Hz, temperature range of 30–150°C at a heating rate of 5°C/min in nitrogen atmosphere, by using a Dynamic Mechanical Analyzer (DMA 2980 model). The dimension of the specimen was 30 × 6.40 × 0.45 mm^3. The reported value of DMA results is based on single time measurement of each sample.

SEM study

A scanning electron microscope (SEM, VEGA II LSU, TESCAN, Czech Republic) was used to study the surface morphology of the solvent immersed pure PMMA and PMMA-clay nanocomposites. Samples were immersed in dichloromethane for 60s and allowed for drying under vacuum at room temperature. Then, the specimens were coated with a thin layer of gold to prevent charging. SEM micrographs were taken at an operating voltage of 10 kv.

RESULTS AND DISCUSSION

Molecular weight determination

The calculated viscosity average molecular weight of pure PMMA and the extracted PMMA in the *in-situ* polymerized PMMA-clay nanocomposites were found to be 28,610 and 20,708, respectively. The decrease in molecular weight of PMMA in presence of clay (polymerization in presence of clay) may be due to the plasticizing effect of the organic modifier presented in the clay. The presence of clay also affects the polymerization kinetics and mechanism that reduce the polymer molecular weight and change its molecular weight distribution.[16]

Wide angle x-ray diffraction (WAXD) study

Figure 1 shows WAXD profiles of the clay itself and the PMMA-clay nanocomposites with 3 wt % clay, prepared by three different manufacturing techniques. The clay itself exhibited the characteristic peak at a 2θ of 3.63°, corresponding to the gallery height (d-spacing) of 2.43 nm (Fig. 1a). The characteristic peak of the clay in all the composites shifted toward lower degree which suggests the intercalation of PMMA chains inside the clay galleries. For solution blended (Fig. 1b, 2θ ~ 2.62°) and direct melt-blended (Fig. 1c, 2θ ~ 2.41°) nanocomposites the clay peak shifted to lower 2θ value with the gallery height of 3.36 nm and 3.66 nm, respectively, consistent with previous results.[11,19,22] The characteristic peak of the clay (2θ ~ 3.63°) was further shifted to lower 2θ region in the *in-situ* polymerized followed by melt-processing (Fig. 1d, 2θ ~ 2.09°) PMMA-clay nanocomposites with the d-spacing of 4.22 nm, which is relatively higher than previously reported[23] with the same clay. The maximum increase in gallery height

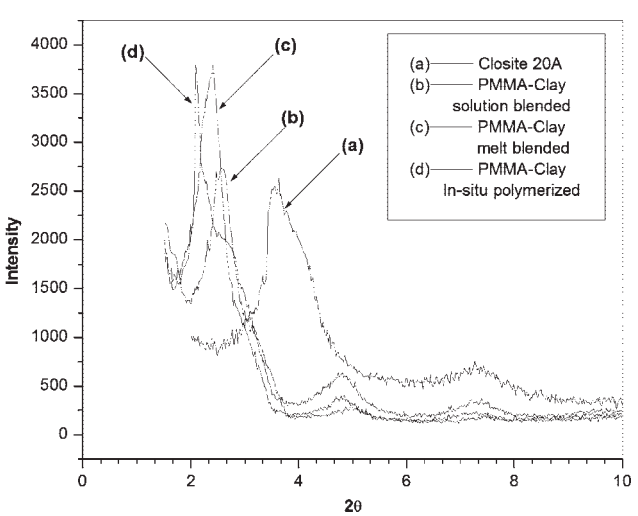

Figure 1 WAXD profiles of the clay itself (a), and the nanocomposites: solution blended (b), melt processed (c), and *in-situ* polymerized (d).

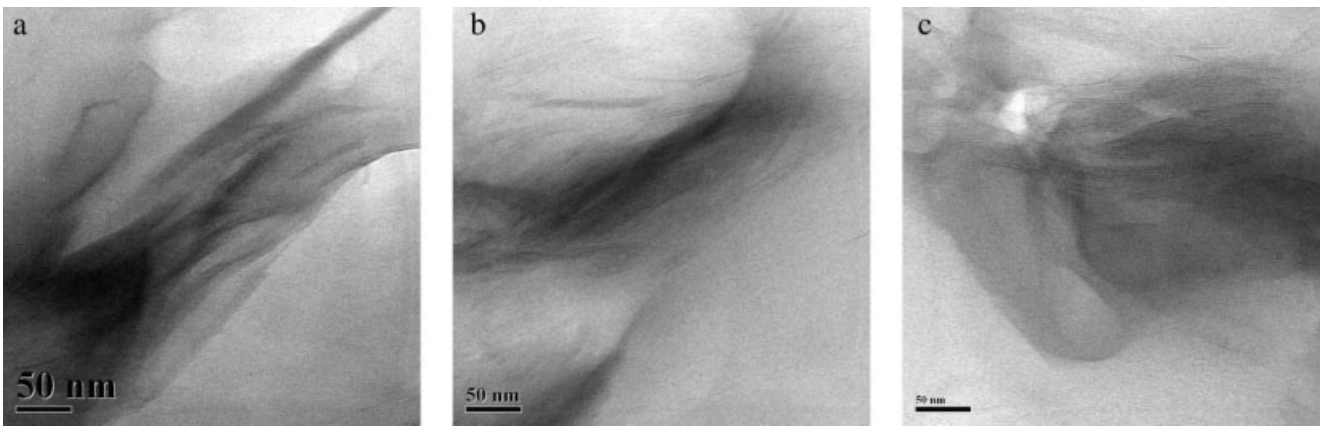

Figure 2 TEM images of the PMMA/clay nanocomposites prepared by the (a) solution blending, (b) direct melt processing method, and (c) *in-situ* polymerization technique. The amount of clay in all the nanocomposites is 3 wt %.

of the clay in case of *in-situ* polymerized PMMA-clay nanocomposite is attributed to the absorption and polymerization of MMA monomers inside the clay galleries.

Viscosity measurement also indicated relatively high viscosity and hence the formation of slightly high molecular weight PMMA in absence of nanoclay. The penetration of PMMA chains inside the clay galleries during melt-mixing becomes difficult with increasing the viscosity of PMMA. This resulted in a relatively poor extent of intercalation (d-spacing) when the PMMA-clay nanocomposites were prepared by direct melt-mixing or solution blending followed by melt-mixing with a relatively high molecular weight PMMA. Whereas, relatively low viscosity of PMMA in *in-situ* polymerized PMMA-clay nanocomposites favours the penetration of PMMA chains inside the clay layers during melt-mixing.

Clay morphology study by transmission electron microscope (TEM)

Figure 2 represents the TEM images of the PMMA-clay nanocomposites prepared by three different methods. Relatively poor extent of intercalation of PMMA chains inside the clay galleries is observed in the solution blended (Fig. 2a) and melt-blended (Fig. 2b) PMMA-clay nanocomposite as compared to the *in-situ* polymerized (Fig. 2c) PMMA-clay nanocomposites. This better intercalation of PMMA in the *in-situ* polymerized PMMA-clay nanocomposite is because of swelling of the clay by MMA monomers and formation of PMMA chains inside the clay galleries. Again, the low viscosity of PMMA in the *in-situ* polymerized PMMA-clay nanocomposite, as indicated by viscosity measurement, also favors the penetration of PMMA chains inside the clay layers during melt-mixing.

Differential scanning calorimetric study

The effect of clay platelet and its extent of dispersion on glass transition temperature (T_g) of PMMA were studied by DSC. Table I represents the T_g values of the neat PMMA and PMMA in the nanocomposites. It is observed that the T_g of neat PMMA (99°C) was shifted to the higher temperature region in the nanocomposites. For example, in PMMA-clay nanocomposites prepared by solution blending and direct melt processing method, the T_g of PMMA shifted to 104°C and 110°C, respectively. This increase in T_g of PMMA in nanocomposites is due to the confinement of PMMA chain inside the clay galleries. The

TABLE I
Glass Transition and Storage Modulus Values of PMMA and its Nanocomposites with 3 wt % of Clay loading, Prepared by Different Manufacturing Techniques

Sample	Glass transition temperature (T_g), (°C)		Storage modulus (GPa)
	DSC	DMA	
Pure PMMA	99	101	1.96
PMMA-clay solution blended	104	107	2.26
PMMA-clay melt blended	110	114	2.42
PMMA-clay *in-situ* polymerized	116	122	2.58

TABLE II
TGA Results of PMMA and its Nanocomposites with 3 wt % of Clay Loading, Prepared by Different Manufacturing Techniques

Sample	T_1 (°C)	T_{50} (°C)	T_{max} (°C)	% wt loss (max)
Pure PMMA	293	351	401	99.40
Solution blended	298	368	408	97.03
Melt blended	321	373	406	96.86
In-situ polymerized	336	388	409	96.74

T_{max}: Temperature corresponds to maximum weight loss.

intercalation of PMMA chains inside the clay gallery restricts the molecular motion of PMMA.[24] Again, the T_g of PMMA was found to be shifted to much higher temperature region (116°C) when the nanocomposite was prepared *by in-situ* polymerization followed by melt intercalation method. Considering the viscosity average molecular weights, the PMMA in *in-situ* polymerized PMMA-clay nanocomposites is expected to show lower T_g value as compared to the melt-blended and solution-blended PMMA-clay nanocomposites. However, maximum increase in T_g of the PMMA was observed in case of *in-situ* polymerized PMMA-clay nanocomposite. This is due to maximum extent of intercalation and hence confinement of PMMA chains inside the clay galleries that restricts the molecular motion of PMMA significantly.

Thermogravimetric analysis

Thermal stability of the pure PMMA and its nanocomposites with 3 wt % of clay has been studied (figure not shown). From the TGA curves, the initial degradation temperature (T_1), temperature corresponds to 50% weight loss (T_{50}) and maximum weight loss (T_{max}) were calculated and shown in Table II. Pure PMMA was found to decompose in two stages, where as in the nanocomposites, the first step disappeared. The slight (~3%) weight loss at ~ 110°C in case of pristine PMMA is related to the "weak links" in the radical-polymerized PMMA as the principal initiation sites of degradation.[25–27] The second steps (considered as onset degradation) in degradation of PMMA are attributed to the presence of head-to-head linkages, the lack of saturation of the end groups related to the combination and termination of two radicals and random scission.

The initial degradation temperature (T_1) and temperature corresponds to 50% weight loss (T_{50}) of neat PMMA shifted to higher temperature region in all the nanocomposites. For instance, the onset degradation temperature (293°C) of neat PMMA increased significantly in the melt processed (321°C) and *in-situ* polymerized (336°C) PMMA-clay nanocomposites. Temperature corresponds to 50% weight loss (T_{50}) of neat PMMA was also increased in all the nanocomposites system with 3 wt % of clay loading. These results indicate improved stability of PMMA against thermal degradation in PMMA-clay nanocomposites that depends on the extent of intercalation, and hence on the method of composite preparation. The significant improvement in thermal stability of relatively low molecular weight PMMA in *in-situ* polymerized PMMA-clay nanocomposites is the result of maximum intercalation of the polymer inside the clay layers.

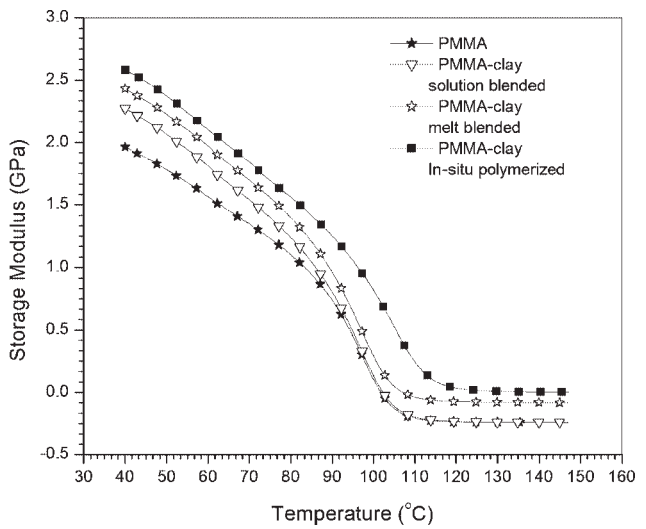

Figure 3 Plot of storage modulus vs. temperature of PMMA (★), and PMMA-clay nanocomposites prepared by solution blending (▽), melt blending (☆), and *in-situ* polymerization (■). The clay loading in all the nanocomposites was 3 wt %.

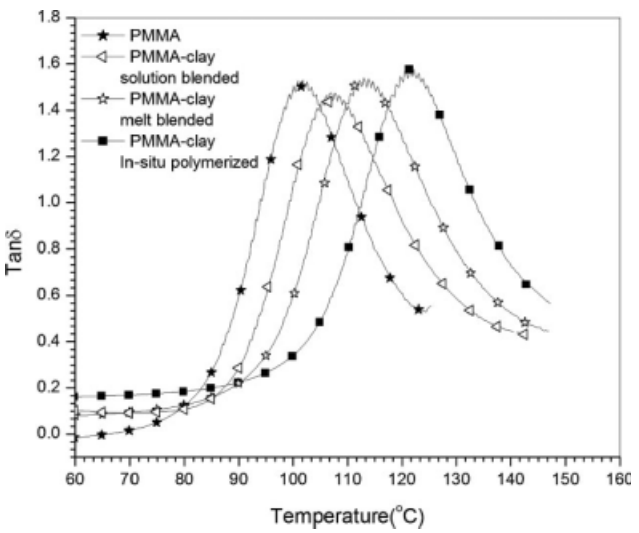

Figure 4 Plot of tanδ vs. temperature for PMMA (★), and PMMA-clay nanocomposites prepared by solution blending (◁), melt blending (☆), and *in-situ* polymerization (■). The clay loading in all the nanocomposites was 3 wt %.

Dynamic mechanical analysis (DMA)

The viscoelastic properties of the pure PMMA and its nanocomposites with 3 wt % of clay, prepared by different methods, were measured as a function of temperature by dynamic mechanical analysis. The storage modulus of the neat PMMA and PMMA-clay nanocomposites are shown in Figure 3. It was observed that in both glassy and rubbery regions, the storage moduli of all the nanocomposites were higher than that of neat PMMA, especially in the elastomeric state. At 40°C, the storage modulus (1.96 GPa) of the neat PMMA was increased to 2.42 GPa and 2.58 GPa for melt blended and *in-situ* polymerized PMMA-clay nanocomposites respectively (Table I). The lower modulus (2.26 GPa) of the solution blended PMMA-clay nanocomposite compared to the *in-situ* polymerized (2.58 GPa) and melt-blended (2.42 GPa) nanocomposites was due to plasticizing effect of the excess surfactant molecules presented in the solution. At the high-temperature region (above T_g), the storage modulus of PMMA-clay nanocomposites was also higher than the neat PMMA. This indicates the reinforcing effect imparted by the high aspect ratio clay platelets that allowed a greater degree of stress transfer at the interface.[28] Furthermore, restricted segmental motion at the organic–inorganic interface due to confinement of the polymeric chains inside the clay galleries at the nanoscale level may be the possible cause for a phenomenal increase in the storage modulus. Thus, the modulus of *in-situ* polymerized PMMA-clay nanocomposites with relatively lower molecular weight PMMA was significantly higher due to maximum extent of clay intercalation as compared to the solution and melt-blended samples.

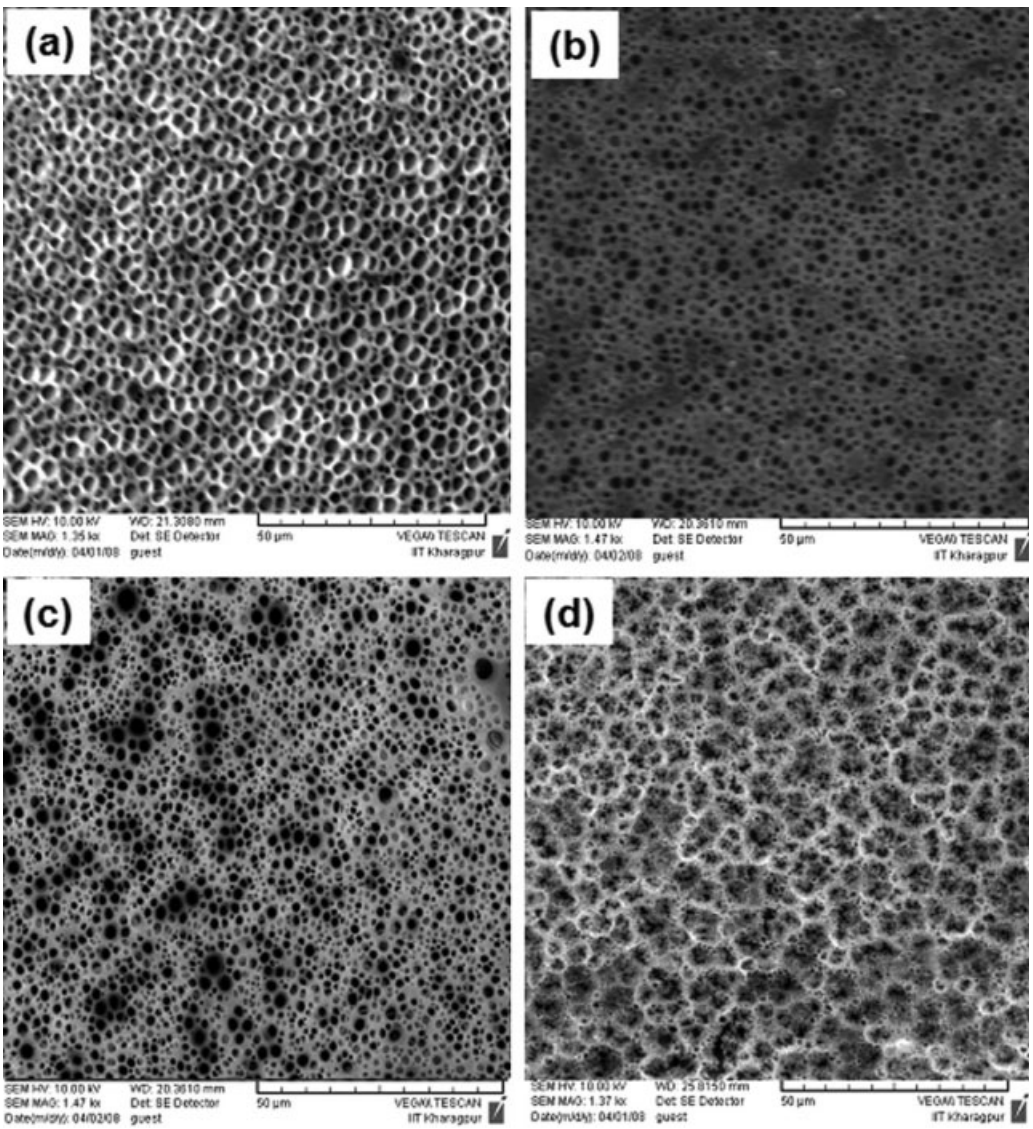

Figure 5 SEM images of the PMMA samples immersed in dichloromethane; (a) Pure PMMA, (b) PMMA-clay Solution Blended, (c) PMMA-clay melt blended, (d) PMMA-clay *in-situ* polymerized.

The variation of tanδ as a function of temperature is shown in Figure 4. The T_g values of pure PMMA and its composites with clay determined from the peak values of tanδ and DSC methods are shown in Table I. From DMA results it is evident that incorporation of clays shifts the T_g of PMMA to higher temperature regions, which are in agreement with the DSC results. This behavior is probably attributed to segmental immobilization of PMMA chains in the presence of nanoscale clay platelets.[29] In the case of *in-situ* polymerized PMMA-clay nanocomposites, significantly higher T_g value was observed as compared with the nanocomposites prepared by the direct melt processing and solution blending with same amount of clay loading. This may be ascribed to the maximum intercalation and confinement of the polymers inside clay layers with better clay dispersion in case of *in-situ* polymerized PMMA-clay nanocomposites that leads to a large surface area of the clay interacting with the polymer chains.

Surface morphology study by SEM

The surface resistance property of the pure PMMA and the PMMA-clay nanocomposites toward solvent molecules were studied using dichloromethane as solvent. The SEM images in Figure 5 represent of the surface morphology of the pure PMMA [Fig. 5(a)], and PMMA-clay nanocomposites [Fig. 5(b-d)] immersed into the solvent for 60s. As observed, the sizes of the holes on the solvent immersed PMMA surface [Fig. 5(a)] decreased significantly in the PMMA-clay nanocomposites. Very fine holes are observed on the surface of the *in-situ* polymerized PMMA-clay nanocomposites [Fig. 5(d)]. This study indicates better surface resistance property of the nanocomposites to prevent dichloromethane from penetrating into the matrix, as compared to that of pure PMMA.[30]

CONCLUSION

The extent of clay intercalation is the key parameter in controlling the properties of the PMMA-clay nanocomposite. For particular clay loading, the extent of dispersion and intercalation of the clay in PMMA matrix was found to depend strongly on the manufacturing techniques. *In-situ* polymerization of the MMA monomers inside the clay galleries resulted in a maximum separation of the silicate layers compared to the melt-intercalation and solution intercalation processes. The possible interactions of the polymer chains with the clay, and hence the improvement in properties of the nanocomposite, depend on the availability of clay platelet surface. XRD results revealed the highest degree of silicate layer separation (gallery height) in *in-situ* polymerized PMMA-clay nanocomposites. Thus, the maximum improvement of thermal stability and storage modulus in the *in-situ* polymerized PMMA-clay nanocomposite indicated significantly higher extent of interaction of PMMA chains with the silicate layer surfaces.

References

1. Zeng, C.; Lee, L. J. Macromolecules 2001, 34, 4098.
2. Manias, E.; Touny, A.; Wu, L.; Strahecker, K.; Lu, B.; Chung, T. C. Chem Mater 2001, 13, 3516.
3. Choi, Y. S.; Wang, K. H.; Xu, M.; Chung, I. Chem Mater 2002, 14, 2936.
4. Kim, Y. K.; Choi, Y. S.; Wang, K. H.; Chung, I. J. Chem Mater 2002, 14, 4990.
5. Wang, D.; Zhu, J.; Yao, Q.; Wilkie, C. A. Chem Mater 2002, 14, 3837.
6. Fu, X.; Qutubuddin, S. Polymer 2001, 42, 807.
7. Okamoto, M.; Morita, S.; Kim, Y. H.; Kotaka, T.; Tateyama, H. Polymer 2001, 42, 1201.
8. Li, X.; Kang, T.; Cho, W. J.; Lee, J. K.; Ha, C. S. Macromol Rapid Commun 2001, 22, 1306.
9. Uhl, F. M.; Wilkie, C. A. Polym Degrad Stab 2002, 76, 111.
10. Vyazovkin, S. I.; Fan, X.; Advincula, R. J Phys Chem B 2004, 108, 11672.
11. Kumar, S.; Jog, J. P.; Natarajan, U. J Appl Polym Sci 2003, 89, 1186.
12. Jiang, G. J.; Tsai, H. Y. Book of Abstract, 219 ACS National Meeting, POLY-402; CA, 2000.
13. Shen, Z.; Simon, G. P.; Cheng, Y. B. Mater Res Soc Symp Proc 1999, Organic/Inorganic Hybrid Materials II 576, 137.
14. Okamoto, M.; Morita, S.; Taguchi, H.; Kim, Y. H.; Kotaka, T.; Tateyama, H. Polymer 2000, 41, 3887.
15. Hwang, K. J.; Kim, D. S. J Appl Polym Sci 2008, 110, 2957.
16. Liqiang, C.; Naresh, T. N. H.; Ihl, W. S. Macromolecules 2008, 41, 4268.
17. Huang, X.; Brittain, W. J. Book of Abstract, PMSE-075, 219 ACS National Meeting; CA, 2000.
18. Sahoo, P. K.; Samal, R. Polym Degrad Stab 2007, 92, 1700.
19. Tiwari, R. R.; Natarajan, U. J Appl Polym Sci 2007, 105, 2433.
20. Rajan, M. A. J.; Mathavan, T.; Ramasubbu, A.; Thaddeus, A.; Latha, V. F.; Vivekanandam, T. S.; Umapathy, S. J Nano Sci Tech 2006, 6, 3993.
21. Akat, H.; Atilla, T. M.; Prez, F. D.; Yagci, Y. Euro Polym J 2008, 44, 1949.
22. Liaw, J. H.; Hsueh, T. Y.; Tan, T. S.; Wang, Y.; Chiao, S. M. Polym Int 2007, 56, 1045.
23. Zeng, C.; Lee, L. J. Macromolecules 2001, 4, 4098.
24. Chang, J. H.; Seo, B. S.; Hwang, D. H. Polymer 2002, 43, 2969.
25. Kashiwagi, T.; Inaba, A.; Brown, J. E.; Hatada, K.; Kitayama, T.; Masuda, E. Macromolecules 1986, 19, 2160.
26. Manring, L. E. Macromolecules 1988, 21, 528.
27. Hu, Y. H.; Chen, C. Y.; Wang, C. C. Polym Degrd Stab 2004, 84, 545.
28. Hasegawa, N.; Okamoto, H.; Kawasumi, M.; Usuki, A. J Appl Polym Sci 1999, 74, 3359.
29. Uthira, K. P.; Song, M. K.; Nah, C.; Lee, Y. S. Euro Polym J 2005, 41, 211.
30. Chen, G.; Chen, X.; Zhiyong Lin, Z.; Ye, W. J Mater Sci Lett 1999, 18, 1761.